International Journal of Mechanical, Industrial and Aerospace Sciences
ISSN: 2517-9950
Vol:2, No:5, 2008

# Fracture Toughness Characterization of Carbon-Epoxy Composite using Arcan Specimen

M. Nikbakht, and N. Choupani

***Abstract*—**In this study the behavior of interlaminar fracture of carbon-epoxy thermoplastic laminated composite is investigated numerically and experimentally. Tests are performed with Arcan specimens. Testing with Arcan specimen gives the opportunity of utilizing just one kind of specimen for extracting fracture properties for mode I, mode II and different mixed mode ratios of materials with exerting load via different loading angles. Variation of loading angles in range of 0-90° made possible to achieve different mixed mode ratios. Correction factors for various conditions are obtained from ABAQUS 2D finite element models which demonstrate the finite shape of Arcan specimens used in this study. Finally, applying the correction factors to critical loads obtained experimentally, critical interlaminar fracture toughness of this type of carbon- epoxy composite has been attained.

***Keywords*—**Fracture Mechanics, Mixed Mode, Arcan Specimen, Finite Element.

## I. Introduction

COMPOSITE structures have been applied in many applications including the aerospace, marine, and civil industries. The ability of these materials to be designed to suit the specific needs for different structures makes them highly desirable. Improvement in design, materials and manufacturing technology enhance the application of composite structures. The suitability of a particular composite material depends on the nature of applications and needs. The technology has been explored extensively for aerospace applications, which require high strength and stiffness to weight ratio materials. [1]

Preventing failure of composite material systems has been an important issue in engineering design. The two types of physical failures that occur in laminated composite structures and interact in complex manner are interalaminar and interlaminar failures. Interalaminar failure is manifest in micro-mechanical components of the lamina such as fiber breakage, matrix cracking, and debonding of the fiber- matrix interface. Generally, aircraft structures made of fiber reinforces composite materials are designed such that the fibers carry the bulk of the applied load. Interlaminar failure such as delamination refers to debonding of adjacent lamina. The possibility that interalaminar and interlaminar failure occur in structural components is considered a design limit, and establishes restrictions on the usage of full potential of composites.

Due to the lack of through-the-thickness reinforcement, structures made from laminated composite materials and adhesively bonded joints are highly susceptible to failure caused by interfacial crack initiation and growth. The delamination phenomenon in a laminated composite structure may reduce the structural stiffness and strength, redistribute the load in a way that the structural failure is delayed, or may lead to structural collapse. Therefore, delamination is not necessarily the ultimate structural failure, but rather it is the part of the failure process which may ultimately lead to loss of structural integrity. Delamination phenomenon caused by exerting compressive loads to structures or buckling is investigated by Reeder [2] experimentally and numerically with using shell elements and a new criterion for initiation of delamination was presented in this research.

There are three basic fracture modes (Fig. 1). Many configurations have been presented for testing the delamination in mode I, mode II and mixed mode condition in literatures. Double cantilever beam (DCB) method in 1989 by Williams for mode I of fracture, End-Notch Flexure (ENF) method by Carlson in 1986 for mode II of fracture and Mixed Mode Bending (MMB) method by Crews and Reeder for first time in 1988 for mixed mode fracture are used to estimate fracture toughness of different materials (Fig. 2). MMB method is modified and use for calculating the critical interlaminar fracture toughness of AS4/PEEK by Reeder in 1990 [3, 4, and 5]. A new apparatus is presented by Szekrenyes [6 and 7] with combining DCB and ENF configurations. The new specimen could be loaded via three point bending machine.

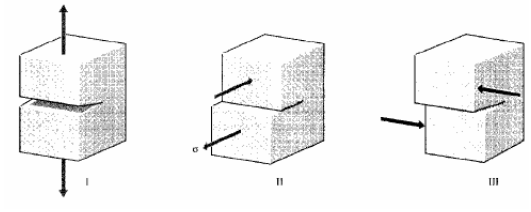


Fig. 1 Fracture modes

Authors are with Department of Mechanical Engineering, Sahand University of Technology, Tabriz, Iran (e-mails: mn_au@hotmail.com, choupani@sut.ac.ir).

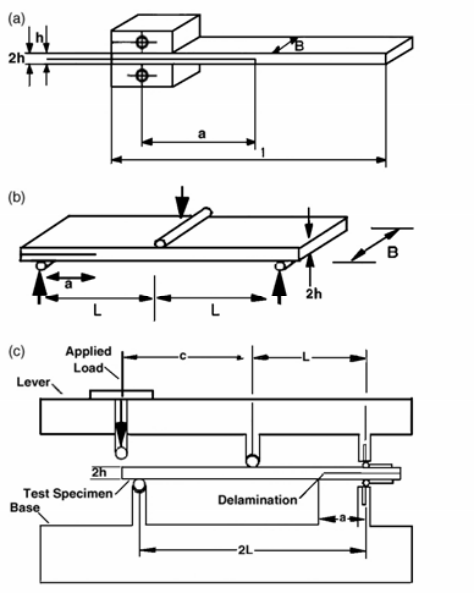


Fig. 2 Interlaminar fracture toughness apparatus (a) mode I double cantilever beam specimen (DCB), (b) mode II end-notch flexure (ENF), (c) mixed mode bending (MMB) specimen

Fracture in mode I, mode II and mixed mode condition and related criterion was investigated by Chao and coworkers [8]. They demonstrated that for the condition when mode I is dominant, hoop stress criterion would predict the fracture well and for the condition when mode II is dominant mechanism in fracture, shear stress criterion can predict the fracture better than the other compared criterions. Priel [9] tested the fracture modes of I and II and mixed mode via three points bending apparatus and compared the results such as critical loads and initiation angle with the related criterion. Results show good agreement with some of these analytical results.

Experimental observation indicates that delamination is usually initiated by high interlaminar stresses at or near geometric discontinuities, material discontinuities, material defects, and interalaminar failures, among other stress raisers. Geometric discontinuities include biomaterial systems; material defects include voids; and interalaminar failures include transverse matrix cracks. If free to do so, each ply of a laminate would deform independently of the other plies due to varying fiber orientation and anisotropy of the laminated composite material. Large stresses at the stress raisers boundaries are necessary to preserve compatible deformations, which are primarily responsible for the nucleation of delamination. The interlaminar stresses at a material (point P) are shown in Fig. 3.

Much of numerical investigations presented in literatures lead to excellent results. These methods are more preferable because of their low cost and time consuming. Finite element models which use 3D shell elements demonstrated good accordance with experimental results [10]. Initiation and propagation of delamination studied numerically with using cohesive elements and different constitutive laws lead to excellent results [11]. In another study which was conducted by Krueger [12] in NASA technical institute, virtual crack closure method for calculation of j integral is investigated with ABAQUS finite element software and validated quantitatively by ANSYS finite element software. This study showed that 20 node quadrilateral elements give the best results.

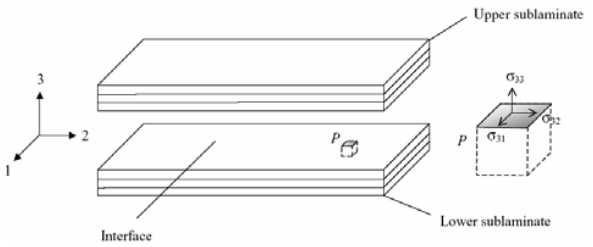


Fig. 3 Interlaminar stresses which are responsible for delamination

For damage tolerance design of composite structures, the critical interlaminar fracture toughness must be calculated previously in order to predict defect growth and hence the strength of the overall structure [1]. In an experiment done via Brazilian Disk, critical interlaminar fracture toughness for Carbon-Epoxy composite fiber with direction of -45/+45 was calculated [13]. In another study, the Brazilian disk was used to calculate the critical fracture toughness of carbon-epoxy composite in different loading conditions and mixed mode ratios and was demonstrated that fracture toughness of mode II is more sensitive to loading speed rather than mode I fracture toughness [14]. Many other researchers such as Prashanat and Verma [15], Kim and Dharmawan [16] calculated the critical fracture toughness of different material via DCB, ENF and MMB apparatus.

Composites are most often classified in terms of their matrix, and are designated as polymer matrix composites (PMCs), metal matrix composites (MMCs), or ceramic matrix composites (CMCs). Although these Systems possess widely different mechanical properties, they experience similar damage accumulation processes. More significantly, although damage introduces a high level of complexity in determining the stress field ahead of a crack tip or a notch, energy-based fracture mechanics concepts allow an elegant means of characterizing the condition for failure, which spans across all the three matrix systems [17]. Typically, the delamination initiates and propagates under the combined influence of normal and shear stresses. Therefore tests of delamination resistance should account for the effects of combined stresses.

The present study addresses delamination testing with combined tensile normal stress (mode I) and sliding shear stress (mode II). Various approaches have been used to develop test specimens with such combined normal and shear stresses on the delamination plane. Unfortunately, however, several types of specimens are often needed to generate delamination toughness data over a desired range of mixed-mode combinations. The pure mode I values for delamination fracture toughness $G_{IC}$ were obtained using a split unidirectional laminate loaded as a double cantilever beam (DCB). The pure mode II values $G_{IIC}$ were found using the

same type of specimen but subjected to three points bending; this type of test is called an end-notch flexure (ENF) test. However, the mode I and mode II components of mixed-mode fracture toughness were generated using cracked-lap shear (CLS) and edge-delamination tension (EDT) specimens. The use of different test configuration can involve different test variables and analysis procedures that can influence test results in ways that are difficult to predict [3].

Arcan specimen for the first time in 1978 was presented for providing plane stress condition in fracture test of mode I, mode II and mixed mode conditions [18]. This apparatus latter was used for developing COD criterion [19]. The influence of finite geometry and type of material is studied by HalBack numerically and experimentally for two types of Aluminum specimens. The fracture behavior and transformation between mode I and mode II is also investigated in this paper [20]. In latter experiments conducted by Ayatollahi and Hong, mode II of fracture is studied separately by this configuration. Yoon also evaluated the fracture toughness of Carbon-Epoxy unidirectional composite with the same specimen [21-23].

In this research correction factors of Arcan specimens are calculated via the Arcan apparatus model in ABAQUS finite element software and critical interlaminar fracture toughness of Carbon-Epoxy cross-ply composite was calculated.

## II. Finite Element Modeling

The stress intensity factors $K_I$, $KII$ and $K_{III}$ play an important role in linear elastic fracture mechanics. They characterize the influence of the of the load or deformation on the magnitude of crack tip stress and strain fields and measure the propensity of crack propagation or the crack driving forces. Furthermore, the stress intensity can be related to the energy release rate (the J-integral) for a linear elastic material through [24]:

$$J = \frac{1}{8\pi} K^T . B^{-1} . K \tag{1}$$

where $K = \begin{bmatrix} K_I & K_{II} & K_{III} \end{bmatrix}^T$ and B is called the pre-logarithmic energy factor matrix. In order to calculate stress intensity factors, interaction integral method is commonly used. In general, the J-integral for a given problem can be written as

$$J = \frac{1}{8\pi}[K_I B_{11}^{-1} K_I + K_I B_{12}^{-1} K_{II} + K_I B_{13}^{-1} K_{III} + (Terms \text{ not involving } K_I)] \tag{2}$$

where *I*, *II*, *III* correspond to 1, 2, 3 when indicating the components of *B*. We define the J-integral for an auxiliary, pure mode I, crack- tip field with stress intensity factor $k_I$, as

$$J_{aux}^I = \frac{1}{8\pi} k_I . B_{11}^{-1} . k_I \tag{3}$$

Superposing the auxiliary field onto the actual field yields

$$J_{tot}^I = \frac{1}{8\pi}[(K_I + k_I) B_{11}^{-1} (K_I + k_I) + 2(K_I + k_I) B_{12}^{-1} K_I + 2(K_I + k_I) B_{13}^{-1} K_{III} + (Terms \text{ not involving } K_I \text{ or } k_I)] \tag{4}$$

Since the terms not involving $K_I$ or $k_I$ in $J_{tot}^I$ are equal, the interaction integral can be defined as

$$J_{\text{int}}^I = J_{tot}^I - J - J_{aux}^I = \frac{k_I}{4\pi}(B_{11}^{-1} K_I + B_{12}^{-1} K_{II} BK + B_{13}^{-1} K_{III}) \tag{5}$$

If the calculations are repeated for mode *II* and mode *III*, a linear system of equation results:

$$J_{\text{int}}^a = \frac{k_\alpha}{4\pi} B_{\alpha\beta}^{-1} K_\beta \tag{6}$$

If the $k_\alpha$ are assigned unit values, the solution of the above equation leads to

$$K = 4\pi B . J_{\text{int}} \tag{7}$$

where $J_{\text{int}} = [J_{\text{int}}^I, J_{\text{int}}^{II}, J_{\text{int}}^{III}]^T$. Based on the definition of the J-integral, the interaction integrals $J_{\text{int}}^\alpha$ can be expressed as

$$J_{\text{int}}^\alpha = Lim_{\Gamma \to 0} \int_\Gamma n . M^\alpha . q d\Gamma \tag{8}$$

with $M^\alpha$ given as

$$M^\alpha = \sigma : \varepsilon_{aux}^\alpha I - \sigma . \left( \frac{\partial u}{\partial x} \right)_{aux}^\alpha - \sigma_{aux}^\alpha . \frac{\partial u}{\partial x} \tag{9}$$

The subscript *aux* represent three auxiliary pure Mode I, Mode II, and Mode III crack-tip fields for $\alpha = I, II, III$, respectively. $\Gamma$ is a contour that lies in the normal plane at position *s* along the crack front, beginning on the bottom crack surface and ending on the top surface (Fig. 4). The limit $\Gamma \to 0$ indicates that $\Gamma$ shrinks onto the crack tip.

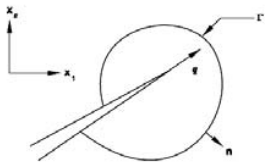

Fig. 4 Contour for calculating J-integral

To evaluate these integrals, ABAQUS [24] defines the domain in terms of rings of element surrounding the crack tip. Different "contours" (domains) are created. The first contour consists of those elements directly connected to crack tip nodes. The next contour consists of the ring of elements share nodes with the elements in the first contour as well as the elements in the first contour. Each subsequent contour is defined by adding the next ring of element that share nodes with the elements in the previous contour [24].

The numerical analysis were performed with ABAQUS finite element software under a constant load of 1000 N. the entire apparatus was modeled using eight node collapsed quadrilateral elements and the mesh was refined around crack tip, so that the smallest element size found in the crack tip

elements was approximately o.25 mm. Linear elastic finite element analysis was performed under a plain strain condition using $1/\sqrt{r}$ stress field singularity. To obtain a $1/\sqrt{r}$ singularity term of the crack tip stress field, the elements around the crack tip were focused on the crack tip and the mid-side nodes were moved to a quarter point of each element side [25].

## III. Experimental Procedure

### A. Overview

The goal of fracture toughness testing is to determine the critical intensity factor or in fact plane strain fracture toughness $K_C$. ASTM standard E399 and D 5054 give some useful information about the plain strain condition and critical plane strain fracture toughness [25]. Due to presence of weak planes between the layers of a composite laminate, interlaminar fracture are often subjected to a mixed mode stress field. The stress intensity factor ahead of the crack tip for modified Arcan specimen was calculated using the following equations [26]:

$$K_I = \frac{P_C\sqrt{\pi a}}{wt} f_1(\frac{a}{w}) \quad (10)$$

$$K_{II} = \frac{P_C\sqrt{\pi a}}{wt} f_2(\frac{a}{w}) \quad (11)$$

where $P_C$ in critical load at fracture, α is loading angle, $w$ is specimen length, t is the specimen thickness and $a$ is crack length. In turn $K_I$ and $K_{II}$ are obtained using geometrical factors $f_1(a/w)$ and $f_2(a/w)$, respectively, which are obtained through finite element analysis of Arcan specimen [25-26].

### B. Materials and Specimen

The aim of the test performed is to determine the critical interlaminar fracture toughness of Carbon-Epoxy thermoplastic composite material. For this purpose, the modified version of Arcan specimen is used. To prepare the specimens by hand layup method, 130 layers of cross-ply carbon laminates each of 0.2 mm thickness and 350 mm length and 50 mm width was put together to form a block with dimension of 350*50*26 mm. To create a precrack in specimens, before hot press step, a layer of teflon with 0.1mm thickness and the dimensions of 25*350mm was inserted between 65th and 66th layer, this layer had the dimensions of 25*350mm. Test specimens as demonstrated in Fig. 5, were machined from prepared block. A noticeable point that must be taken into consideration is the specific shape of this specimen, many researchers had complained about the complex procedure of joining the specimen to main apparatus. Adhesive joints are more used in many experiments but steps of preparing two parts and adherent need so much time and cost and also employing advanced equipments is needed. Furthermore, these kinds of joints have very low resistance against shear forces and using them in Mode II fracture test may lead to unreliable results. Thus, for the reasons mentioned above specimens are machined with the shape of Fig. 6. Elastic constant of Carbon-Epoxy used in this investigation is summarized in Table I. The direction 1 and 2 are in crack plane and 3 is the direction transverse to the crack plane.

TABLE I
Elastic Properties of Carbon-Epoxy Laminated Composite

| | |
|---|---|
| $E_1$(GPa) | 37.05 |
| $E_2$(GPa) | 37.05 |
| $E_3$(GPa) | 7.6 |
| $G_{12}$(GPa) | 5 |
| $G_{13}$(GPa) | 2.76 |
| $G_{23}$(GPa) | 2.76 |
| $\nu_{12}$ | 0.04 |
| $\nu_{13}$ | 0.36 |
| $\nu_{23}$ | 0.36 |

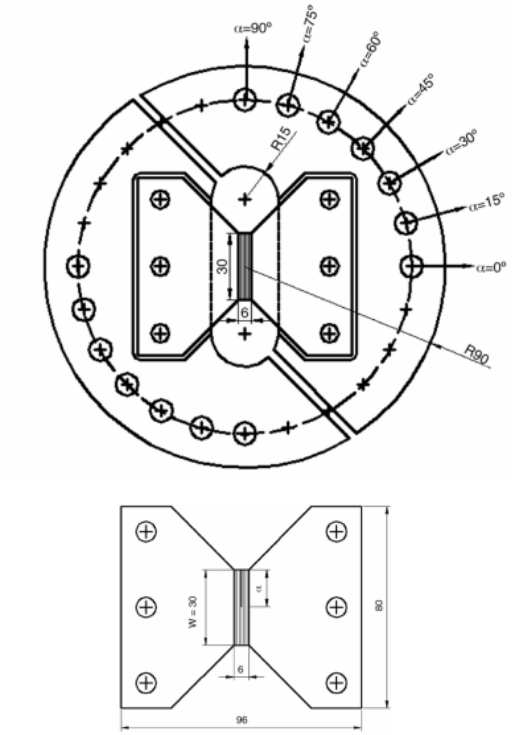


Fig. 5 Fixture and Arcan specimen

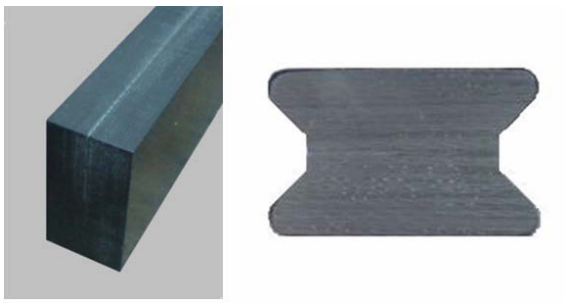

(a) (b)

Fig. 6 (a) Primitive specimen, (b) Specific machined specimen

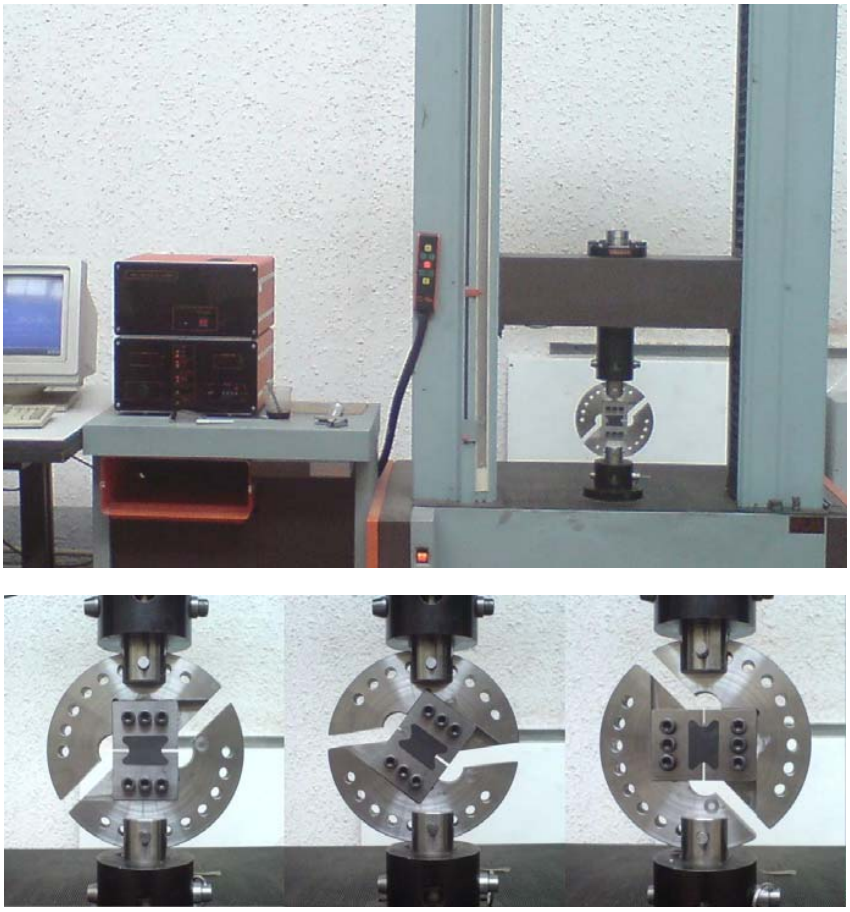

(a) (b) (c)

Fig. 7 An overview of loading device and setup: (a) pure mode I; (b) mixed mode; (c) pure mode II

### C. Test and Setup

Arcan specimen and apparatus is showed in Fig. 7. Fixture is made of BOZ-6582 high tensile steel with Thickness of 20mm and machined in the way to be able to test a 10mm specimen. The holes created in circumference make loading in various angles possible. Loading was carried out with a tensile loading device with the rate of 0.5mm per minute until the final rapture. To reduce the effected of involved errors, loading in each angle was repeated 3 times and the average value was counted as final rapture load or critical load.

## IV. Results and Discussions

### A. Mixed-mode Interlaminar Fracture Specimen Calibration

For determining fracture toughness from (10) presented in previous chapter, non dimensional stress intensity factor which is shown with $f(a/w)$ is calculated numerically for Arcan specimen and demonstrated in Fig. 8. In this diagram $a/w$ is the ratio of crack length to specimen thickness.

In Fig. 9 the stress intensity factor $f(a/w)$ for pure mode I and pure mode II is demonstrated versus different loading angles. It can be seen for loading angles less than 58 degree, mode I is dominant system of fracture and for more than 58 degree mode II is dominant. The contribution of mode-I have decreased by increasing of loading angle and simultaneously, the contribution of mode-II increases and also it can be seen that for $\alpha \geq 60$ , mode-II becomes dominant.

### B. Mixed-Mode Interlaminar Fracture Toughness

The interlaminar fracture toughness was determined experimentally with the modified version of the Arcan specimen under different mixed-mode loading conditions. The average values of mixed-mode interlaminar critical stress intensity factors for Carbon-Epoxy composite are summarized in Table II. $(K_I)_C$ remains almost unchanged until $\alpha = 45^\circ$ and then decreases and $(K_{II})_C$ increases as the mode-II loading contribution, i.e. as α increases from $0^\circ$ to $90^\circ$. It is seen that for loading angles $\alpha \leq 60$, the mode-I contribution is greater than that of mode-II and the opening-mode fracture becomes dominant. For loading angles $\alpha \geq 60$ there is an opposite trend and the shearing mode fracture become dominant. For

loading angle between $60^\circ$ and $75^\circ$ there is not enough experimental information but, as said previously and can be seen in Fig. 6, shifting the dominant mode of fracture from opening mode to shearing mode occurs in about $68^\circ$ thus for loading angle of $75^\circ$, mode-II becomes dominant, also, fracture toughness of mode-I and mode-II that is demonstrated in Table III show a good accordance with this numerical results. From Table III, it can be seen that the shearing-mode ($\alpha = 90^\circ$) interlaminar fracture toughness is larger than the opening-mode ($\alpha = 0^\circ$) interlaminar fracture toughness. This means that the interlaminar cracked specimen is tougher in shear loading conditions and weaker in tensile loading conditions.

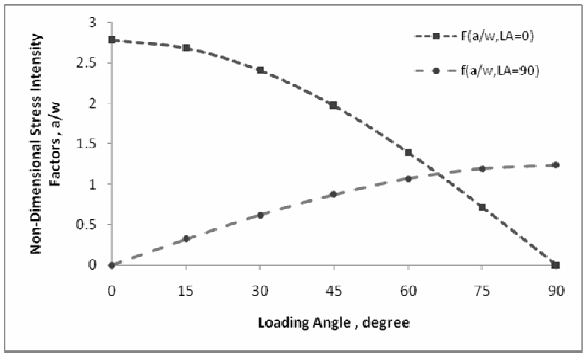


Fig. 8 Non-dimensional stress intensity factor vs. loading angle of Carbon-Epoxy composite for the crack length 15mm.

The average values of interlaminar fracture toughness in terms of stress intensity factors for Carbon-Epoxy composite material under pure mode-I and pure mode-II loading are summarized in Table III. Interlaminar fracture toughness measurement for the modified Arcan specimen under pure mode-I loading show the average fracture toughness of $K_{IC} = 0.97(MPa.m^{1/2})$ for Carbon-Epoxy composite material. For pure mode-II loading using modified Arcan specimen, the average fracture toughness for Carbon-Epoxy composite material was found $K_{IiC} = 1.89(MPa.m^{1/2})$.

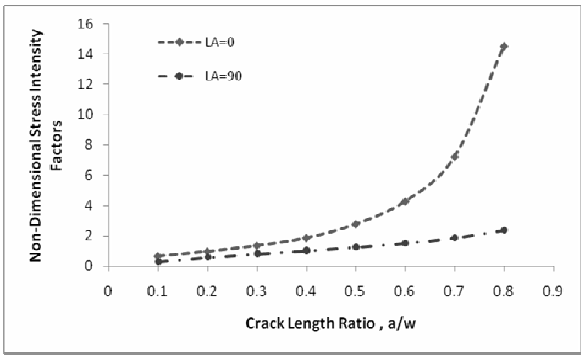


Fig. 9 Non-dimensional stress intensity factors vs. crack length of Carbon-Epoxy composite material

TABLE II
AVERAGE CRITICAL MIXED-MODE INTERLAMINAR FRACTURE LOADS $P_C$ (N) FOR CARBON-EPOXY COMPOSITE WITH CRACK LENGTH 15MM

| | | Loading Angles | | | | | | |
|---|---|---|---|---|---|---|---|---|
| | | 0 | 15 | 30 | 45 | 60 | 75 | 90 |
| **Critical Loads** | 1 | 480 | 540 | 560 | 730 | 1080 | 1800 | 2200 |
| | 2 | 480 | 480 | 600 | 710 | 1210 | 1820 | 1980 |
| | 3 | 490 | 520 | 610 | 725 | 1150 | 1730 | 2150 |
| **Average** | | 483.33 | 513.33 | 590 | 721.67 | 1146.67 | 1783.34 | 2110 |

TABLE III
AVERAGE INTERLAMINAR CRITICAL STRESS INTENSITY FACTORS ($K_C$) ($MPa\ m^{1/2}$) FOR CARBON-EPOXY COMPOSITE WITH CRACK LENGTH 15MM

| | | Loading Angles | | | | | | |
|---|---|---|---|---|---|---|---|---|
| | | 0 | 15 | 30 | 45 | 60 | 75 | 90 |
| **Fracture Toughness** | $K_{IC}$ | 0.985 | 0.997 | 1.028 | 1.027 | 1.154 | 0.925 | |
| | $K_{IIC}$ | | 0.118 | 0.264 | 0.456 | 0.888 | 1.541 | 1.888 |

## V. Conclusion

In this paper the mixed-mode interlaminar fracture behavior of Carbon-Epoxy composite specimens was investigated based on experimental and numerical analyses. A modified version of Arcan specimen was employed to conduct a mixed mode test using the special test loading device. The full range of mixed-mode loading condition including pure mode-I and pure mode-II loading can be created and tested. It is a simple test procedure, clamping unclamping the specimens is easy to achieve and only one type of specimen is required to generate all loading conditions.

The finite element results indicate that for loading angles close to pure mode-II loading, a high ratio of mode-II to mode-I fracture is dominant and there is an opposite trend for loading angles close to pure mode-I loading. It confirms that by varying the loading angle of Arcan specimen pure mode-I, pure mode-II and a wide range of mixed-mode loading condition can be created and tested. Also, numerical results confirm that the increase of the mode-II loading contribution leads to an increase of fracture resistance in the Carbon-Epoxy composite and the increase of the crack length leads to a reduction of interlaminar fracture resistance in the Carbon-Epoxy composite.

The interlaminar fracture toughness was determined experimentally with the modified version of the Arcan specimen under different mixed-mode loading condition. Results indicated that the interlaminar cracked specimen is tougher in shear loading condition and weaker in tensile loading condition.

## References

[1] F. Dharmawan, G. Simpson, I. Herszberg, S. John. “Mixed mode fracture toughness of GFRP composites.” Composite Structures,2006
[2] James R. Reeder. K. Song, P. Chunchu, D. R. Ambur, “Postbukling and growth of delamination in composite plates subjected to axial compression.” AIAA journal, 2002.
[3] James R. Reeder and John R. Crews. “Mixed Mode Bending Method for Delamination Testing.” Published in AIAA Journal, vol 28, 1990, pages 1270-1276.
[4] James R. Reeder. “3d mixed mode delamination fracture criteria-an experimentalist perspective.” NASA Langley research center,M/S 188E, Hampton VA 23681-2199,USA.
[5] John H. Crews, Jr. and James R. Reeder. “A mixed mode bending apparatus for delamination testing.” NASA technical memorandum 100662, August 1988.
[6] Andras Szekrenyes. “Delamination fracture analysis in the GI-GII plane using prestressed transparent composite beams.” International journal of solids and structures 44(2007) 3359-3378.
[7] Andras Szekrenyes. “Prestressed fracture specimen for delamination testing of composites.” International journal of fracture (2006) 139: 213-237.
[8] Yuh J. Chao and Shu Liu. “On the failure of crack under mixed mode loads.” International journal of fracture 87: 201-223, 1997.
[9] E. Priel, A. bussiba, I. Gilad, Z. Yosibash. “Mixed mode failure criteria for brittle elastic V-notched structures.” International journal of fracture (2007) 144: 247-265.
[10] Ronald Krueger. “A shell/3D modeling technique for delamination in composite laminates. In proceedings of the American society for composites,” 14th technical conference, technomic publishing, 1999.
[11] Ronald Krueger, P. J. Minguet, T. K. O’Brien. “Implementation of interlaminar fracture mechanics in design: an overview.”, Presented at 14th international conference on composite materials (ICCM-14), San Diego, July 14-18,2003.
[12] R. Krueger, D. Goetze. “influence of finite element software on energy release rates computed using the virtual crack closure technique.” NASA/CR-2006-214523, NIA Report No. 2006-06.
[13] C. Liu, Y. Huang, M.L. Lovato, M.G. Stout. “measurement of the fracture toughness of fiber reinforced composite using the Brazilian geometry.” International journal of fracture 87: 241-263.1997.
[14] L. Banks-Sills, Y. Freed, R. Eliasi, V.Fourman. “fracture toughness of the +45/-45 interface of laminate composite.” International journal of fracture (2006) 141: 195-210.
[15] S.K. Verma, P. Kumar. “Evaluation of critical sif of DCB specimen made of slender cantilever. Engineering fracture mechanics.” 1995.
[16] B.W. Kim, A.H. Mayer, “Influence of fiber direction and mixed mode ratio on delamination fracture toughness of carbon-epoxy laminates.” Composite science and technology. 2003.
[17] B.S. Majumdar and D. Hunston, “Continuous Parallel Fiber Composites: Fracture”, Encyclopedia of Materials: Science and Technology, Elsevioe Ltd. 2001.
[18] M. Arcan, Z. hashin, A. voloshin, “A method to produce uniform plane stress state with application to fiber-reinforced materials,” Experimental mechanics. 1978.
[19] M.A. Sutton, W. Zhao, M.L. Boone, A. P. Reynolds, D.S. Dawicke, “Prediction of crack growth direction for mode I/II loading using small-scale yielding and void initiation/growth concepts.” International Journal of Fracture, 83, 1997.
[20] N. Hallback. “The influence of finite geometry and material properties on mixed mode I/II fracture of aluminum.” International journal of fracture 87: 151-188, 1997.
[21] M.R. Ayatollahi, R. Hashemi. “Mixed mode Fracture in an inclined center crack repaired by composite patching.” Composite structure, 81, 264-273, 2007.
[22] M.R. Ayatollahi, D.J. Smith and M.J. Pavier.“Crack-tip Constraint in mode II deformation.” International Journal of Fracture, 113, 2002.
[23] S.C. Hung and K.M. Liechti. “An evaluation of the Arcan specimen for determining the shear module of fiber reinforced composites.” Experimental mechanics, volume 37, no. 4, December 1997.
[24] ABAQUS user’s manual, version 6.5. Pawtucket, USA: Hibbit, Karlsson and Sorensen, HKS Inc; 2004.
[25] American society for testing and materials.1991,standard D5045-91a,plane-stain fracture toughness and strain energy release rate of plastic materials, Annual book of ASTM standards Philadelphia: ASTM.
[26] N. Choupani. “Experimental and numerical investigation of the mixed mode delamination in Arcan laminated specimens.” Material science and technology, volume 478(2008): 229-242.